An Examination of the Feasibility of Using OpenFOAM to Model Air Flow for Wind Turbine Positioning

Dan Holdaway, Gavin Tabor and Bob Beare
College of Engineering, Mathematics and Physical Science, University of Exeter

Contents

Thanks to Tradewind Turbines, Exeter, UK for supporting this project and for providing access to their wind turbine.

1 Introduction

Wind energy is now becoming a vital component of global electricity production. Large scale wind farms composed of many hundreds of wind turbines are being built all around the World to help meet the energy demands of the population whilst alleviating carbon dependency. In addition to this large scale production of energy it is also possible for individuals to place their own wind turbines and generate their own electricity. When placing wind turbines, whether they be part of huge offshore wind farms or in the back garden, some important considerations need to be taken into account. Generating the maximum amount of energy from any given wind turbine relies on careful consideration of its surrounding environment; it needs to be placed somewhere where the airflow is clean and consistent rather than turbulent or being blocked by surrounding objects. If the air passing the turbine exhibits turbulence or is blocked in some way then the driving mechanism of the turbine will not work efficiently and production rate estimates will likely be inaccurate. Indeed Johnson (2008) attribute a 5% overestimate of wind farm production rates due to lack of understanding of meteorological phenomena.

Wind flow near the surface of the Earth, and within the wake of wind turbines, can be highly complex and exhibit turbulent behaviour; as a result it is not always clear on the best location for a wind turbine. If building a wind farm then consecutive turbines should be placed far enough apart so that wake from upstream turbines does not affect the flow across downstream turbines. This of course is just one constraint amongst many that need to be considered by wind farm engineers. Large scale wind farms are generally built in large open areas or out at sea where airflow is clean, reliable and where local interactions need not be considered. When one wishes to use a wind turbine on a smaller scale, such as to power their home or business, there is likely to be much greater restriction on the choice of placement. Indeed one would be likely to choose a location where local effects such as surrounding buildings or vegetation will interfere with the wind flow; the surrounding terrain is also likely to be less uniform than in the locations chosen for large scale wind farms. Local structures and complicated terrain will cause turbulence in the wind and will even block the wind completely in localised regions. These additional considerations make it quite a challenge to optimise the position of even a single turbine.

One of the problems when considering the location of individual wind turbines within built up, hilly or vegetated areas is the complexity of the local wind flow. As air flows past a building or tree it will likely exhibit some level of turbulence in the downstream wake, or may be completely blocked. Turbulent flow, by its very nature, is difficult to predict and the effect it has on a wind turbine is even harder to predict. Due to the eddies in the flow it is likely that overall turbulence will have

an adverse effect on turbine operation, therefore wind turbines should generally be placed in regions where flow is least turbulent. However a further consideration is that a region that is ideal in one wind direction may not be in another wind direction. The side of a hill may seem a good location; when the wind blows up the side of that hill it is known to accelerate, however in the opposite wind direction the turbine would be placed in the wind shadow of the hill.

Due to the complexity of airflow, particularly around small scale structures and the large variations in wind conditions it would be highly time consuming to analyse a candidate turbine location by measuring weather conditions. Instead a tool that is likely to be useful is computational fluid dynamics (CFD). In CFD the Navier-Stokes equations of fluid flow are modelled using state of the art finite volume methods and adaptive mesh techniques. This allows one to set up realistic simulations of all kinds of wind flow conditions, whilst also incorporating complex terrain and surrounding vegetation and buildings through the state of the art meshing tools. Modelling of wind turbine wake is crucial when building large scale wind farms as and has been addressed using CFD by a number of researches, see Vermeer et al. (2003) for an overview. So far less attention has been directed towards simulating wind flow for a local area with turbine positioning in mind. As technology improves and energy costs rise there is likely to be an increase of people and businesses who wish to purchase a turbine and produce their own power. If a picture of the local wind can be accurately predicted, and thus an optimal site for the turbine site be provided, then it is likely that the efficiency of the turbine will increase.

1.1 Computational Fluid Dynamics

In CFD the Navier-Stokes equations of fluid flow are modelled; these equations are capable of describing all of the processes, including turbulence, exhibited by the flow. Except in idealised cases it is not possible to perform a direct numerical simulation (DNS) of the Navier Stokes equations and capture all relevant scales; there will thus always be unresolved processes in the flow. Instead of DNS some turbulence model is considered that estimates the effect of these unresolved processes on the resolved part of the flow. Popular techniques for simplifying the governing equations so that unresolved processes can be more easily considered include Reynolds averaging of the Navier-Stokes (RANS) and large eddy simulation (LES). In RANS the complexity of the equations are reduced by performing a time averaging; in LES the equations are spatially averaged. Both methods require a turbulence model, sometimes known as a subgrid model, to capture the terms left over from the averaging which are sub grid scale. Many turbulence models exist and again each have different advantages and disadvantages. An important

consideration when performing CFD is in choosing the appropriate technique and subsequent turbulence model for the problem being considered.

1.1.1 OpenFOAM

A number of CFD applications exist, most of which are commercial. CFD software is generally very flexible and can be applied to any number of numerical problems, from airflow across an aerofoil to modelling heat flow in a combustion engine. Within the component designed for modelling airflow a number of 'out of the box' turbulence models are available for both RANS and LES. OpenFOAM, standing for Open Field Operation and Manipulation, is an open source CFD toolbox that is completely free to use. That the software is open source makes it a very attractive option for modelling atmospheric flow for wind turbine placement. Despite the flexibility of the CFD toolboxes available many of the turbulence models are designed with engineering specific problems in mind and are lacking in atmospheric specific variations. The open source nature of OpenFOAM means it can be adapted until models capable of capturing the features of the atmosphere are obtained.

1.2 The Atmospheric Boundary Layer

One of the issues when attempting to model atmospheric flow using a CFD toolbox is in capturing the atmospheric boundary layer. When one examines the boundary layer when air flows past an aerofoil, for example, a very thin boundary layer is found. However the atmospheric boundary layer can be much deeper, up to the order of 1km. It is not clear that an atmospheric boundary layer type wind profile will be properly maintained by the turbulence models readily available in OpenFoam or any other CFD toolbox. The structure and depth of the atmospheric boundary layer is governed by shear driven turbulence which is either suppressed or enhanced by stratification and hence the boundary layer evolves with a diurnal cycle. During the day the surface warms and in turn heats the air closest to the surface; this warmer less dense air then travels convectively upwards to regions of higher density cooler air, producing a turbulent region up to the order of 1km deep. As the sun begins to set the surface cools and the air in the boundary layer becomes stably stratified, i.e. with cool air below warm air. The stable stratification acts to suppress the shear generated turbulence and the overall turbulent region shrinks down to the order of a few hundred metres. The deeper daytime boundary layer is referred to as the convective boundary layer while the shallower nocturnal boundary layer is known as the stably stratified boundary layer. A further neutral case can occur where the temperature is constant throughout the depth of the boundary layer. For simulating wind flow for turbine positioning it is important to capture

the atmospheric boundary layer wind profile accurately, however it is possible to do this without considering the stratification. Provided a realistic wind profile can be maintained in neutral conditions it will be sufficient for describing the optimal position for the turbine.

Reynolds averaging is commonly used for describing the turbulence in the atmospheric boundary layer and is currently used in the unified model at the UK Met Office, Lock et al. (2000). In the Met Office model, and in many other operational weather forecast models, a turbulence closure is used for the Reynolds stresses that is specifically designed to capture the properties of the atmospheric boundary layer. Due to the large differences between the diurnal stages of the boundary layer different closures are used for daytime and nightime. One of the most commonly used turbulence models in the CFD toolboxes is the $k-\epsilon$ closure which relates the transport due to turbulent eddies to the turbulent kinetic energy k and the dissipation of kinetic energy ϵ. This is in contrast to the standard Met Office approach of using mixing length (stable) and surface flux (convective). However the use of kinetic energy in the closure is not uncommon in meteorological applications, such as the TKE closure, Beljaars (1992).

A number of authors have explored the use of CFD software with the $k-\epsilon$ closure for capturing valid atmospheric boundary layer wind profiles. Richards and Hoxey (1993) were among the first to demonstrate some appropriate adaptations to the closure parameters and this has been followed up by Hargreaves and Wright (2007), who implemented the changes of Richards and Hoxey (1993) for modern CFD applications Fluent and CFX. Further work has been also been done in implementing the adaptations of Richards and Hoxey (1993) in an OpenFOAM simulation, e.g. Sumner and Masson (2009). In these studies it is shown that CFD applications using the $k-\epsilon$ can properly model a neutral boundary layer profile. A useful guide to CFD modelling of atmospheric boundary layers over complex terrain is provided by Franke et al. (2007).

The overall aim of this work is to determine whether it would be possible to construct a wind flow simulation over a realistic complex terrain with realistic buildings and vegetation within OpenFOAM. The results of the simulation can then be used to provide information about the optimal location for a wind turbine in that region. The first stage of achieving this goal will be to construct a CFD simulation which can model boundary layer wind profiles that are derived from both analytical functions and realistic data. This will involve adapting the OpenFOAM model to take into account the requirements set out by authors such as Richards and Hoxey (1993) or Yang et al. (2009). The work of Richards and Hoxey (1993) is based on a 2D analysis and does not take complex terrain into account and so the extent to which results for these cases extends to 3D modelling of complex terrain

needs to be considered. A further factor that will be considered here is the wind turning that occurs in the boundary layer and the effect that this can have on the choice of wind turbine placement.

Work of this nature lies at the intersection of a number of complex disciplines: atmospheric boundary layer modelling, turbulence modelling, flow over complex terrain and computational fluid dynamics. In order to generate useful results it will be necessary to draw on the expertise from all of these disciplines, making this a highly multi-disciplined problem. The aim of this project is to establish whether a simulation over complex terrain is possible using OpenFOAM, not necessarily to perform and complete and accurate simulation. In the process of examining the required steps to simulate flow over complex terrain it is likely that a number of questions will be identified that will need to be addressed in future efforts.

2 The Equations to be Modelled

Fluid flow problems of this nature begin with the incompressible Navier-Stokes equations, which are given by,

$$\frac{D\mathbf{u}}{Dt}+\frac{1}{\rho}\nabla p = \nu\nabla^2\mathbf{u}, \tag{1}$$

$$\nabla.\mathbf{u} = 0. \tag{2}$$

These coupled equations represent the conservation of momentum and conservation of mass. The equations are highly nonlinear and are capable of representing all the scales possible in a fluid flow problem. Due to the large range of scales in fluid flow problems and the limitations in computational capability the equations require some simplification on order to make progress towards a solution. Here the simplification will be made by performing a Reynolds averaging.

The Reynolds averaged Navier-Stokes equations are found by writing all model variables as their mean plus fluctuating parts, i.e. $u = U + u'$. Terms can then be time-averaged to gain an insight to the overall flow property. It is assumed that for a certain period of time the fluctuating parts average to the mean flow i.e. $\overline{U + u'} = \overline{U}$, the averaging period is assumed long enough that fluctuations average to the mean flow, but not so long that the mean flow itself could be evolving. The property of the averaging is thus $\overline{u'} = 0$ and thus that $\overline{u} = \overline{U}$. Note however that nonlinear products of fluctuating variables, e.g. $\overline{u'u'}$, do not go to zero, indeed these are required for modelling turbulence which is an inherently nonlinear process. After performing the averaging, and dropping the overline notation on averaged

mean terms for simplicity, equations (1) - (2) become,

$$\frac{D\mathbf{U}}{Dt} + \frac{1}{\rho}\nabla P = \nu\nabla^2\mathbf{U} - \frac{\partial\left(\overline{u'u'}\right)}{\partial x} - \frac{\partial\left(\overline{u'v'}\right)}{\partial y} - \frac{\partial\left(\overline{u'w'}\right)}{\partial z}, \tag{3}$$

$$\nabla.\mathbf{U} = 0. \tag{4}$$

Note that for a Newtonian fluid Reynolds stresses become, e.g. $\left(\overline{u'v'}\right) = \tau_{xy} = \nu_t\left(\frac{\partial u}{\partial y} + \frac{\partial v}{\partial x}\right)$ and then that equation (3) reduces to,

$$\frac{D\mathbf{U}}{Dt} + \frac{1}{\rho}\nabla P = \left(\nu + \nu_t\right)\nabla^2\mathbf{U}. \tag{5}$$

2.1 $k-\epsilon$ Closure

All terms in equation (5) are known except ν_t, which is unresolved and must be found using a closure. As discussed above, a popular method in engineering applications and readily available in CFD software, such as OpenFOAM, is the $k-\epsilon$ closure, which approximates ν_t as,

$$\nu_t = C_\mu\frac{k^2}{\epsilon}. \tag{6}$$

The constant C_μ is usually taken as $C_\mu = 0.09$. k is the turbulent kinetic energy and ϵ is the dissipation of turbulent kinetic energy. In computing the $k-\epsilon$ closure equations for k and ϵ must be evaluated, these equations are,

$$\frac{\partial k}{\partial t} + \nabla.k\mathbf{U} = \left(\nu + \frac{\nu_t}{\sigma_k}\right)\nabla^2 k + G - \epsilon, \tag{7}$$

$$\frac{\partial \epsilon}{\partial t} + \nabla.\epsilon\mathbf{U} = \left(\nu + \frac{\nu_t}{\sigma_\epsilon}\right)\nabla^2\epsilon + C_{1\epsilon}G\frac{\epsilon}{k} - C_{2\epsilon}\frac{\epsilon^2}{k}. \tag{8}$$

The constants are defined as $\sigma_k = 1.00$, $\sigma_\epsilon = 1.3$, $C_{1\epsilon} = 1.44$, $C_{2\epsilon} = 1.92$ and the production rate of turbulence is given by,

$$G = \nu_t\left(\nabla\mathbf{U} + \nabla\mathbf{U}^{\mathrm{T}}\right)^2. \tag{9}$$

The derivation of the $k-\epsilon$ closure is a highly complex procedure and solving the equations numerically is equally complex. A further advantage of CFD applications however is that the complex numerics are largely already in place and so only relatively minor changes need to be made before the simulation can be performed. It is however important to have a feel for the closure and how it works to ensure accurate and useful simulations are performed.

In OpenFOAM the equations of the flow, with the relevant closure, are solved

using a finite volume solver. In OpenFOAM there are large number of options available for the numerical schemes that can be used and these can be seen in the readily available documentation and within the source code.

3 Atmospheric Boundary Layer Wind

As described in the introduction the boundary layer can be either stably stratified, convective (unstably stratified) or neutrally stratified. For each type of stratification the wind profile will vary. Typically a stable boundary layer will have a jet like profile where the highest speed wind occurs somewhere between the top of the boundary layer and the ground. A convective boundary layer is more likely to have wind speed increasing throughout the boundary layer region. Examples of nocturnal and convective boundary layer structures can be seen in Beare et al. (2006) and Beare (2008). These examples are recreated and shown in Figure 1.

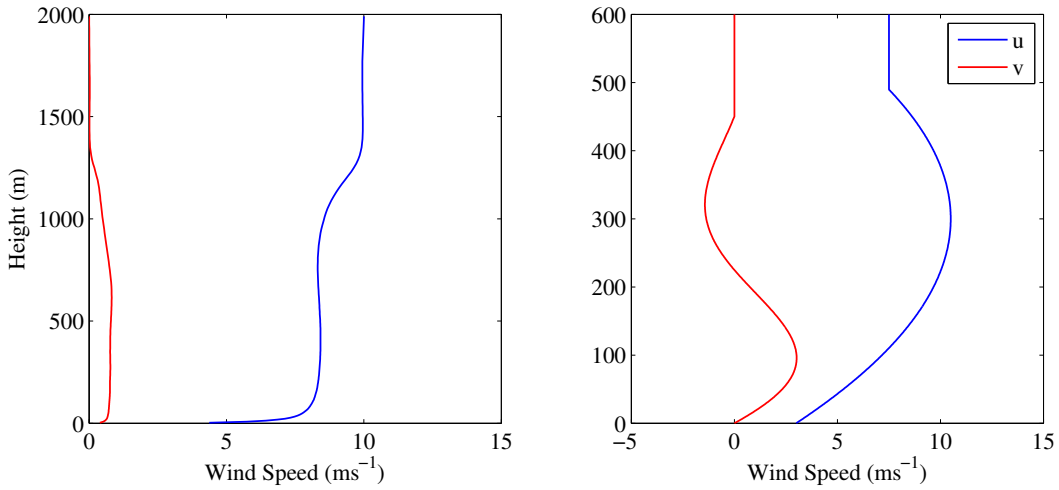

Figure 1: Examples of wind speed profiles for the convective (left) and stable nocturnal (right) atmospheric boundary layers.

It is clear from Figure 1 that the stable boundary layer exhibits the jet feature, peaking here at approximately 300m. For the convective boundary layer the u component of the velocity increases throughout the depth of the boundary layer. The top of the boundary layer in the convective case is at approximately 1400m, the top of the boundary layer in the stable case is approximately 500m. In both cases there is a Coriolis induced turning in the wind, which can be recognised by the presence of a v component. In a situation where only a boundary layer is being considered the coordinate can be transformed so that above the boundary layer $v = 0$. Surface boundary conditions for the atmospheric boundary layer are not imposed directly at the surface but through a roughness length z_0. This roughness length is a parameter that is tuned according to the terrain, whether

the environment be open water, fields, forest or urban. Typically it may vary from around 0.01m up to a few meters.

Whether the boundary layer be stable or unstable observations suggest that near the ground the velocity has a log like scaling $u \sim \ln\left(\frac{z}{z_0}\right)$. Within this surface layer velocity can be approximated by,

$$U = \frac{u_\star}{\kappa} \ln\left(\frac{z + z_0}{z_0}\right), \tag{10}$$

where $\kappa = 0.41 \pm 0.1$ is the von-Karmen constant and $u_\star$ is the friction velocity.

In terms of wind turbine modelling it can be sufficient to consider the wind to have structure given by equation (10) throughout since the wind turbine is situated in the region in which this is a valid approximation. In order to compute $u_\star$ the equation is rearranged with a value for velocity U^{ref} at a given height H^{ref},

$$u_\star = \frac{U^{\text{ref}}\kappa}{\ln\left(\frac{H^{\text{ref}}+z_0}{z_0}\right)}. \tag{11}$$

Values of U^{ref} and H^{ref} are chosen so as to give appropriate wind speeds.

It is clear from Figure 1 that if equation (10) is adapted so that $U = U^{\text{ref}}$ if $z >= H^{\text{ref}}$ a good approximation for the convective boundary layer wind speed may be obtained up to a height of around 800m. (10) gives a simplified view of the structure of the wind in the boundary layer, it would not be capable of reprenting say the nacturnal jet seen in the above figure. The function can be adapted to capture more complex behaviour by taking into account the stratification, e.g. Beljaars (1992).

4 Obtaining a Horizontally Homogeneous Solution.

The work of Richards and Hoxey (1993) is motivated by the requirement that any boundary layer model should, in the absence of complex terrain, be capable of producing a horizontally homogeneous solution. That is that the profiles of all prognostic variables should be the same at any point in the downstream flow as they are upstream. If this were not the case it would be difficult to establish the kind of profile being solved by the turbulence model since the solution far downstream is independent of the inlet profile and only determined by the form of the turbulence closure. In addition to the ability of the model to capture a horizontally homogeneous solution Blocken et al. (2007) note that a CFD simulation of the atmospheric boundary should have the following properties:

- That the grid should have sufficient resolution close to the ground.
- That the distance from the ground to the mid point of the near ground cell z_p should be greater than the physical roughness K_s of the terrain.
- That the model employs a clear relationship between physical roughness K_s and aerodynamics roughness z_0.

However, as pointed out by Blocken et al. (2007), it is currently not possible to achieve all four of these requirements. High resolution near the ground and the present understanding of the relationship between K_s and z_0 can lead to K_s much larger than z_p, this leads to inaccuracies which result in streamwise gradients in the flow and thus a solution that is not horizontally homogeneous.

Capturing a horizontally homogeneous flow is clearly the key issue. Without this property in the model one cannot assume that any simulation of a realistic terrain or environment will be accurate. Wind speeds predicted by the model will be incorrect and this will likely lead to inaccuracies in the predicted wind flow approaching a turbine location and thus how much energy that turbine will produce. In a way the points on the above list are there to produce an accurate horizontally homogeneous and therefore useful simulation.

Before one sets out trying to obtain a horizontally homogeneous solution it is first important to understand the kind of structure that the atmospheric boundary layer should have. Profiles for the velocity are required as well as the components of the chosen closure. If the $k-\epsilon$ closure is to be used then the structures of k and ϵ for the corresponding velocity profile need to be understood and described. Richards and Hoxey (1993) were among the first to consider how the $k-\epsilon$ closure should be implemented for atmospheric boundary layer flow simulation. They were able to generate analytical profiles for k and ϵ based on the well known log profile for the velocity. They then set about describing ways in which the wall functions used in the closure should be adapted so that these analytical profiles could be retained throughout the domain.

Hargreaves and Wright (2007) produced an important piece of work that effectively modernised the work of Richards and Hoxey (1993). They show very clearly how the ideas presented in Richards and Hoxey (1993) could be implemented into modern CFD software, making the results highly accessible. The work concentrates on providing the appropriate form for the shear stress, the production rate of turbulent kinetic energy G and the dissipation rate of kinetic energy in the cell closest to the ground.

The Richards and Hoxey (1993) approach is based on adapting the wall functions to improve the streamwise solution. However this is not the only approach, Blocken et al. (2007) consider the relationship between K_s and z_0, Yang et al. (2009)

concentrate on adapting the inlet profiles to match what the closure is doing and O'Sullivan et al. (2011) consider the boundary conditions implemented at the top of the domain. It is not necessarily that one approach is the best and indeed it may be that some combination of the approaches offered by these authors will lead to the most accurate modelling.

The four approaches for obtaining a horizontally homogeneous solution can be summarised as,

- Adapt the wall functions implemented by the CFD software so that the closure can capture the analytical inlet profiles. Hargreaves and Wright (2007); Richards and Hoxey (1993); Sumner and Masson (2009).
- Adapt the roughness implementation. Blocken et al. (2007)
- Adapt the inlet profiles to something with closer resemblance to wind tunnel experiments and closer resemblance to the type of profile solved by the current wall functions. Yang et al. (2009).
- Adapt the top boundary conditions to allow the flow to exit and enter the domain and suit the closure. O'Sullivan et al. (2011).

Three approaches are discussed and compared here, Richards and Hoxey (1993), Yang et al. (2009) and O'Sullivan et al. (2011).

4.1 Richards and Hoxey (1993) Approach

The analytical profiles described by Richards and Hoxey (1993) are,

$$U = \frac{u_\star}{\kappa} \ln\left(\frac{z + z_0}{z_0}\right), \tag{12}$$

$$k = \frac{u_\star^2}{\sqrt{C_\mu}}, \tag{13}$$

$$\epsilon = \frac{u_\star^3}{\kappa(z + z_0)}. \tag{14}$$

They note that equations (12)-(14) form a solution to two dimensional versions of equations (7) and (8) but only when

$$\sigma_\epsilon = \frac{k^2}{(C_{1\epsilon} - C_{2\epsilon})\sqrt{C_\mu}} \tag{15}$$

so an updated version of σ_ϵ is used with these analytical profiles. The constant $u_\star$ is computed using (11) which leads to inlet profiles for U, k and ϵ as well as the constant σ_ϵ. The wall functions are then updated so they become more suited

toward capturing these profiles. The updated wall functions are described clearly in a modern CFD context by Hargreaves and Wright (2007).

The comparison performed by Hargreaves and Wright (2007) is performed using Fluent; the Fluent wall functions that they update compute the stress at the surface and the production and dissipation of turbulent kinetic energy at the surface. The way these terms are computed using Fluent is very similar to the standard way in which they are implemented in OpenFOAM. In order to implement the updated wall functions in Fluent Hargreaves and Wright (2007) write a series of User-Defined Scalars. In OpenFOAM it is considerably easier to implement the changes since the program is open source. The wall functions for k, ϵ and ν_t can be accessed directly and adapted to suit the alternative form, as can the inlet boundary conditions for U, ϵ and k.

In addition to the updated wall functions Richards and Hoxey (1993) advise that a constant shear stress of $\tau = \rho u_\star^2$ is applied at the top of the domain in the streamwise direction. It also seems sensible to apply values of k and ϵ given by the analytical profiles at the top of the domain, although this is not directly implied by Hargreaves and Wright (2007), who appear, like others, to use a slip boundary condition for these values.

4.2 Yang et al. (2009) Approach

The Yang et al. (2009) approach differs in that they assume the standard wall functions to be accurate but argue that the inlet profiles for k and ϵ need to be adapted. They also show that these adapted inlet profiles give a more accurate representation of profiles obtained from wind tunnel experiments. The Yang et al. (2009) analytical profiles for kinetic energy and dissipation of kinetic energy are,

$$k = \frac{u_\star^2}{\sqrt{C_\mu}} \sqrt{Y_1 \ln\left(\frac{z + z_0}{z_0}\right) + Y_2}, \tag{16}$$

$$\epsilon = \frac{u_\star^3}{\kappa(z + z_0)} \sqrt{Y_1 \ln\left(\frac{z + z_0}{z_0}\right) + Y_2}. \tag{17}$$

The main downside to this approach is that the constants Y_1 and Y_2 are obtained by fitting profiles to realistic data. This introduces an extra amount of work before the profiles can be used for a given situation and means the method lends itself less straightforwardly to a flow over complex terrain.

4.3 O'Sullivan et al. (2011) Approach

O'Sullivan et al. (2011) describe a set of consistent top boundary conditions. In

addition to the constant shear stress described by Richards and Hoxey (1993) they suggeest that the flow should be allowed to exit and re-enter the domain at the top boundary by implementing fixed gradient boundary conditions on k and ϵ. These conditions are found by differentiating equations (13) and (14) or (16) and (17). For the Yang et al. (2009) solution the top boundary conditions would be,

$$\frac{\partial k}{\partial z} = \frac{1}{(z+z_0)} \frac{Y_1}{\sqrt{\left(Y_1 \ln \frac{z+z_0}{z_0}\right) + Y_2}}, \tag{18}$$

$$\frac{\partial \epsilon}{\partial z} = \frac{-u_\star^3}{\kappa (z+z_0)^2} \left[\frac{Y_1}{\sqrt{\left(Y_1 \ln \frac{z+z_0}{z_0}\right) + Y_2}} - \sqrt{\left(Y_1 \ln \frac{z+z_0}{z_0}\right) + Y_2} \right]. \tag{19}$$

Equivalent top boundary conditions for the Richards and Hoxey (1993) approach are found by setting $Y_1 = 0$ and $Y_2 = 1$ in equations (18) and (19).

4.4 Comparison of Approaches

Clearly there are a number of possible approaches to ensuring that the solution will be horizontally homogeneous and so it is useful to compare some of them. In the following the two general approaches of Richards and Hoxey (1993) and Yang et al. (2009) are compared. In order to do this a domain is constructed that has dimensions 5000m$\times$10m$\times$500m in the x, y and z directions. In the y direction there are no grid points, creating a two dimensional simulation. In the z direction levels are staggered so as give higher resolution close to the ground. With a given set of boundary and initial conditions the equations are iterated to steady state using the SIMPLE algorithm. Provided profiles of the model variables are equivalent at the inlet and at 5000m downstream then the solution can be thought of as being horizontally homogeneous. Figure 2 shows the model domain.

The boundary conditions need to be specified at the inlet ($x = 0$m), at the top of the domain ($z = 500$m), at the outlet ($x = 5000$m), and at the ground ($z = 0$). The solution can be considered periodic in y. Boundary conditions are required for $U = (u, v, w)$, k, ϵ, ν_t and p. In addition to value of the model variables at the boundaries OpenFOAM also requires the user to specify the initial internal field for each parameter. At the inlet realistic atmospheric profiles for U, k and ϵ are provided by either Richards and Hoxey (1993) or Yang et al. (2009); ν_t is calculated and pressure is set by $\frac{\partial p}{\partial z} = 0$. At the top of the domain either basic slip conditions are employed on all variables or U, k and ϵ are given fixed values based on the inlet profiles or the consistent boundary conditions of O'Sullivan et al. (2011) are used. At the outlet $\frac{\partial}{\partial x}(U, k, \epsilon, \nu_t) = 0$ and p is allowed to vary with the internal field.

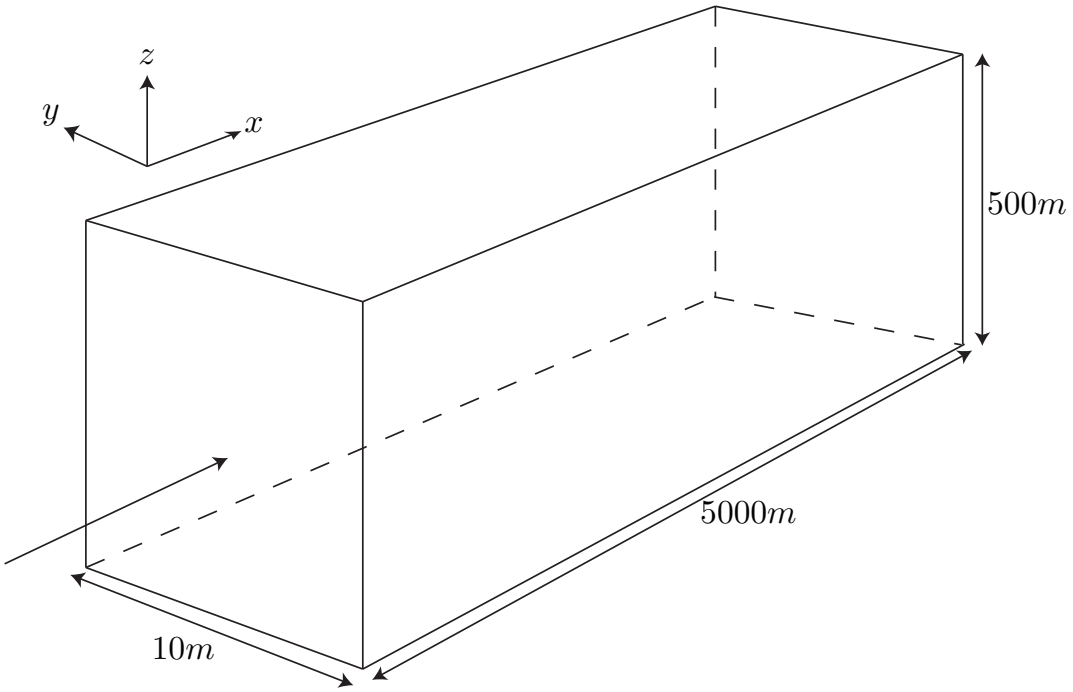

Figure 2: The model domain (not to scale).

At the ground $U = (0, 0, 0)$ and $\frac{\partial p}{\partial z} = 0$; either the standard OpenFOAM rough wall functions are used for k, ϵ and ν_t or the ϵ and ν_t wall functions are adapted to match those described by Richards and Hoxey (1993). Other variables that are used to generate the atmospheric profiles are $\kappa = 0.41$, $H_{\text{Ref}} = 6\text{m}$, $U_{\text{Ref}} = 10\text{ms}^{-1}$, $z_0 = 0.01$ and $\nu = 10^{-5}$.

In Figure 3 the Richards and Hoxey (1993) approach is considered. The figure shows the analytical profiles for U, k and ϵ as given by Richards and Hoxey (1993) and also shows the profiles at $x = 4900\text{m}$ from the simulation. Included is the difference between the $x = 4900\text{m}$ velocity profile and the analytical profile, giving an indication of how well the configuration performs. In the left column of the figure the profile across the whole domain is shown and in the right hand column only the lowest part of the domain is shown. Wind turbines range in height from around 5m up to around 120m so it is important to capture the near ground velocity accurately in any simulation. All results shown in Figure 3 are computed using the Richards and Hoxey (1993) inlet profiles, the various plots show the effect of updating from the standard CFD setup to the Richards and Hoxey (1993) setup. Firstly the effect of using the proper formualtion of σ_ϵ, then the effect of the updated wall functions with either the standard slip top boundary condition, the Richards and Hoxey (1993) top boundary conditions or the O'Sullivan et al. (2011) top boundary conditions.

To gauge the difference between these configurations consider the velocity error plots, which show the difference between the downstream velocity profile and the

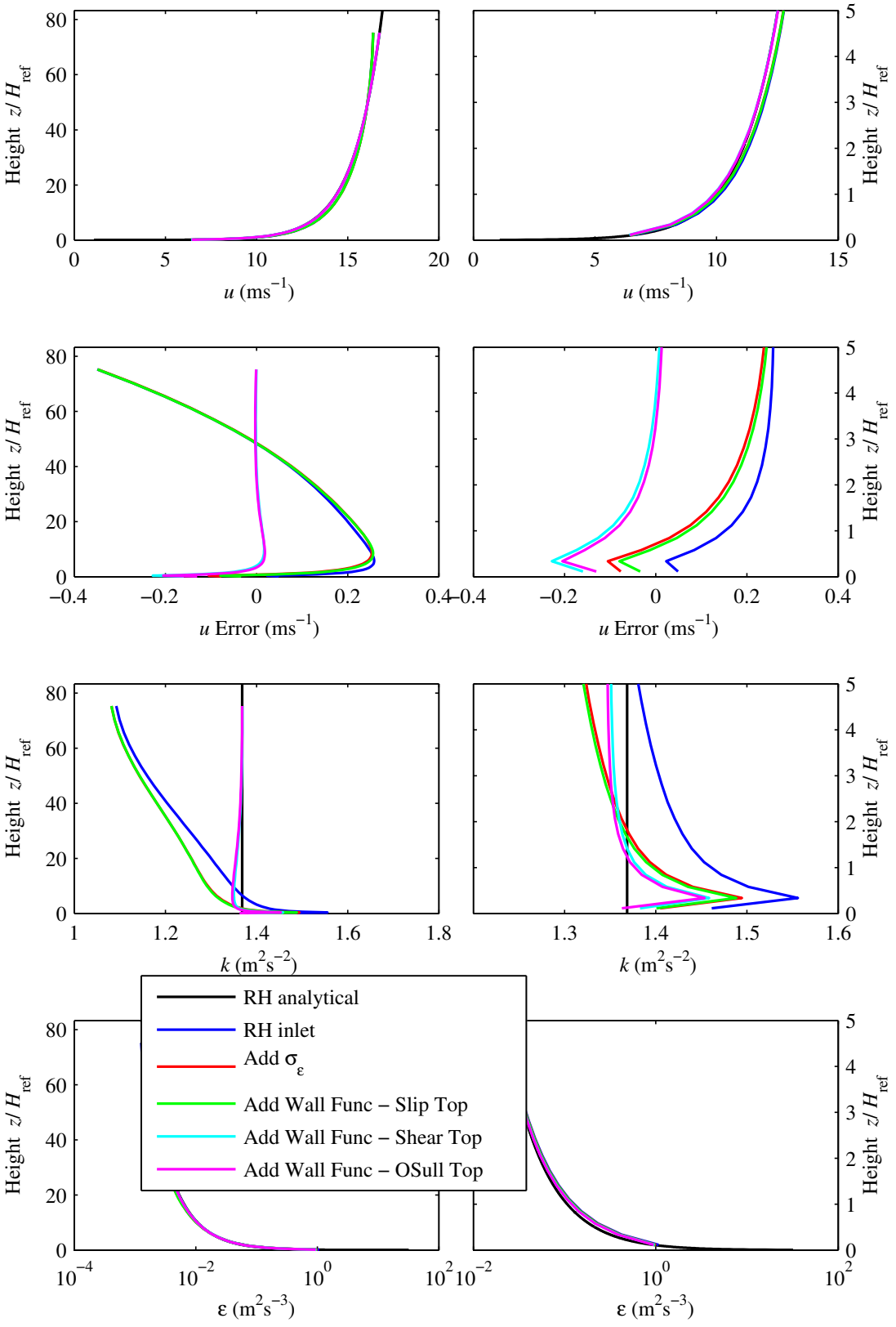

Figure 3: Downstream profiles of velocity, error in velocity, ϵ and k using the Richards and Hoxey (1993) approach to producing a horizontally homogeneous solution. The left column shows the whole domain the right column shows the lowest 30m of the domain.

analytical profile. If the value is negative it means wind speed is under predicted, if positive then over predicted. It is clear that across the domain as a whole it is the updated top boundary condition which has the largest benefit. The downstream profile is very close to the analytical profile everywhere except in the lowest 8m-10m. In the very lowest part of the domain ($z/H_{\text{Ref}} < 1$) the configuration which uses the Richards and Hoxey (1993) wall functions with the standard slip boundary condition at the top of the domain is gives the most accurate wind speed.

Figure 4 shows downstream versus analytical profiles when using the Yang et al. (2009) approach. Here the inlet profiles for k and ϵ are given by (16) and (17); the constants Y_1 and Y_2 are -0.01 and 1.23 respectively, as given by O'Sullivan et al. (2011). Fortunately O'Sullivan et al. (2011) repeated the tests of Yang et al. (2009) but for the same U_{ref} and H_{ref} values used by Hargreaves and Wright (2007), this allows for a clear comparison without the arduous task of finding Y_1 and Y_2. In Figure 4 the Yang et al. (2009) inlet profiles are used in conjunction with the standard slip top boundary conditions as well as the O'Sullivan et al. (2011) consistent top boundary conditions. In this case the wall functions are just the standard OpenFOAM/Fluent versions since the Yang et al. (2009) inlet profiles are designed to work with this standard setup.

It is clear from the figures that top boundary conditions are an important aspect. Throughout the entire domain the configuration with the consistent top boundary conditions gives the least difference between the downstream velocity profile and the analytical velocity profile. It can also be seen that the use of the Yang et al. (2009) inlet profiles in conjunction with the O'Sullivan et al. (2011) consistent top boundary conditions gives a smaller discrepancy between analytical and downstream velocity profiles than any of the configurations shown in Figure 3.

For performing any simulation of the atmospheric boundary layer it is likely that the Yang-O'Sullivan setup will give the most accurate results - at least over flat terrain. There is one clear disadvantage to this technique however, that one must pin down the constants Y_1 and Y_2, which is not done automatically but instead by fitting the analytical profile to some experimental data or idealised case. This is a potential disadvantage given the range of inlet profiles that may be required to do a comprehensive study for locating wind turbines or wind farms. Its use would also need to be investigated when the terrain is nonuniform and values such as z_0 and $u_\star$ are not necessarily fixed throughout the domain.

These tests are all performed using $\kappa = 0.41$, as is the OpenFOAM standard. In Hargreaves and Wright (2007) a value of $\kappa = 0.4$ is used instead. It is also useful to just check how large an affect a change of this magnitude in κ will have. Figure 5 shows streamwise velocity errors for configurations which use Richards and Hoxey (1993) inlet profiles, σ_ϵ, top boundary conditions and wall functions

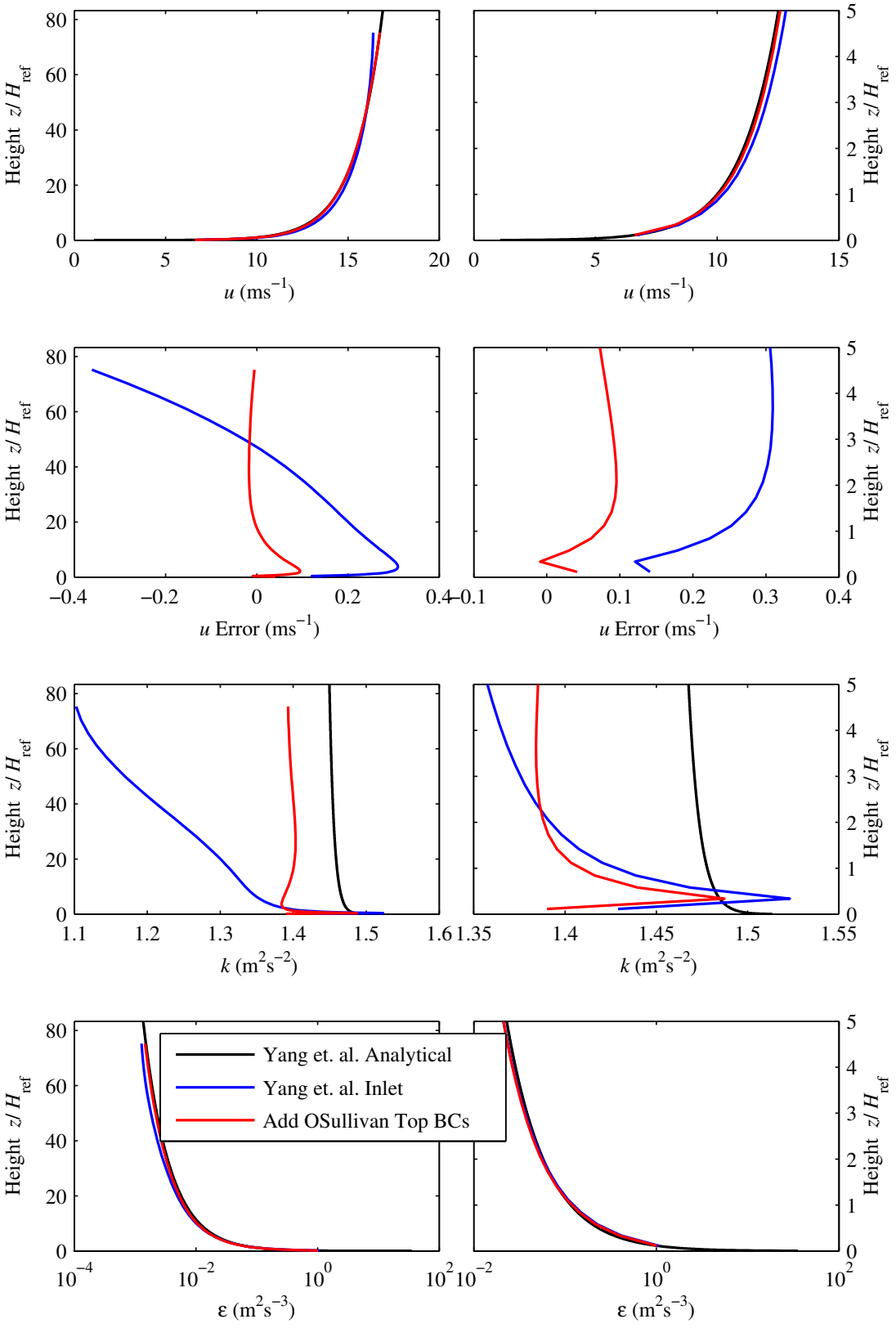

Figure 4: As for Figure 3 except solutions generated using the Yang et al. (2009) approach. The figure demonstrates the Yang et al. (2009) approach on its own as well as the combination of the Yang et al. (2009) and O'Sullivan et al. (2011) approaches.

with both $\kappa = 0.4$ and $\kappa = 0.41$. Using $\kappa = 0.4$ instead of $\kappa = 0.41$ makes the solution slightly more accurate but the difference between the configurations is relatively small. A similar test for Yang et al. (2009) profiles is not possible without recomputing Y_1 and Y_2.

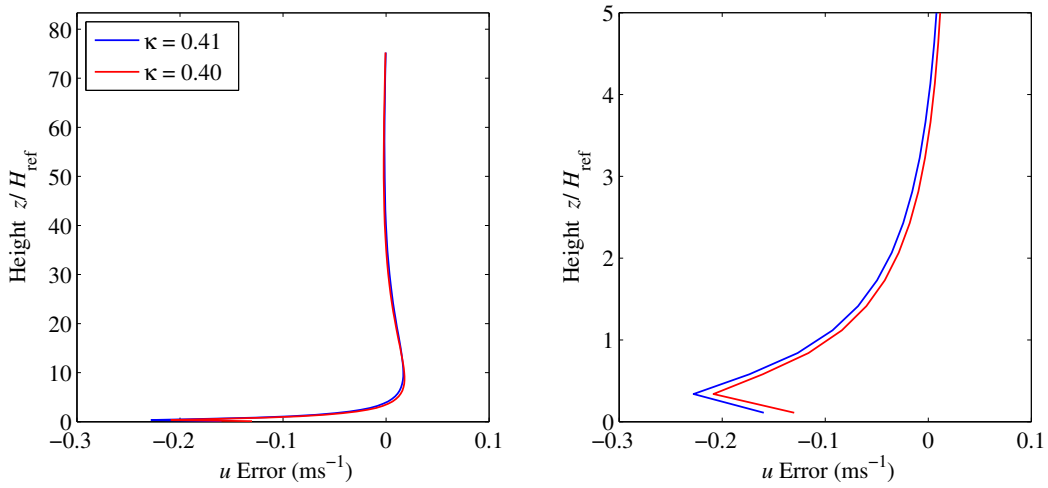

Figure 5: Comparison between using $\kappa = 0.41$ and $\kappa = 0.4$ for a Richards and Hoxey (1993) configuration.

5 Using realistic Inlet Profiles

It would be useful if future simulations involving complex terrain could be used in conjunction with readily available atmospheric data such as the Met Mast data. This may be useful for producing a more realistic inlet profile for the given terrain. As discussed above however the solution that is captured by the turbulence model is somewhat independent of the inlet conditions; if a long enough domain is used then the downstream part of the flow is independent of the upstream part of the flow. This can be seen in Figure 6. The figure shows the solutions both upstream and downstream when using the Beare et al. (2006) stable boundary layer initial conditions for the inlet profile. Clearly the inlet profile is not maintained downstream, the turbulence model is attempting to capture a profile that looks like equation (10), which does not simultaneously describe the stable boundary layer profile. The only way to capture any of a realistic profile would be to first fit a profile like equation (10) to the realistic data and use as an inlet condition. However it would be difficult to match the two profiles for more than just small region and the majority of the structure would not be maintained.

As outlined in the introduction a purpose of this work is to identify some interesting issues that could be addressed in future work on CFD of atmospheric boundary layers. Maintaining a realistic profile could make for quite an interesting

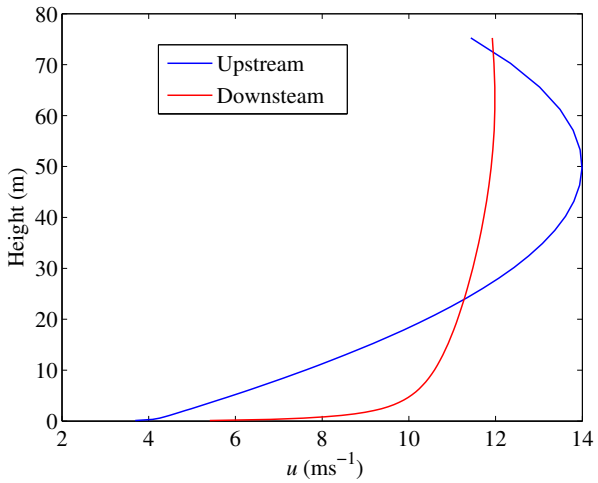

Figure 6: Upstream versus downstream profiles when the inlet boundary condition is given by the Beare et al. (2006) stable boundary layer profile.

project as it would be very useful if the CFD model could be forced by realistic wind profiles, as opposed to just the theoretical logarithmic profile. There would certainly be some interesting questions regarding how the turbulence model should be constructed. It seems likely that the current $k - \epsilon$ model would need some overhaul so that it could recreate any profile, or it may be that another type of closure, such as mixing length, would be more appropriate. A further question is on the use of stratification, currently models employ a neutral stratification and so do not solve for the temperature. It might be useful to add an equation for a further thermodynamic variable enabling the consideration of the stratification. Considering stratification would be particularly useful if one wished to study the transition between stable and convective boundary layers that occurs at dawn and dusk.

6 Implementing Complex Terrain

Now that it has been shown that OpenFOAM and the $k - \epsilon$ closure can be used to obtain a horizontally homogeneous solution that supports atmospheric type profiles it needs to be determined whether it can also be employed for a realistic complex terrain case. There are a number of issues that need to be considered before a simulation can be conducted. Firstly a complex terrain needs to be implemented and meshed using OpenFOAM and secondly it needs to be shown that the equations and closure construction can generate accurate solutions around complex terrain and on complex meshes. Testing would generally need to be done in a systematic way using simplified models and test cases. Usually these tests may consist of, for example, flow past a two or three dimensional bump or flow past a site for

which much data has been collected. An example of a simple test case is that of flow past a cosine bump, as considered by Ishihara and Hibi (2002); Ishihara et al. (1999); Stangroom (2004). Common examples of locations for which realistic data is available are The Askervein Hill project, Taylor and Teunissen (1983, 1985) and The Bolund Hill experiment, Bechmann et al. (2009). The Bolund Hill experiment has been used to perform blind comparisons of competing CFD codes.

6.1 Verifying the Turbulence Model

Unfortunately a detailed examination of various test cases and comparison with realistic terrain is beyond the scope of this feasibility study. However it is demonstrated briefly that OpenFOAM can indeed be used to perform these kinds of studies. The case that is considered here is the cosine bump case as described and cited by Stangroom (2004). The hill is described by,

$$z = \begin{cases} h\cos^2\left(\pi\frac{\sqrt{x^2+y^2}}{2L}\right) & \sqrt{x^2+y^2} \leq L \\ \\ 0 & \text{otherwise} \end{cases}, \tag{20}$$

where $h = 40m$ is the height of the hill and $L = 2.5L$. The hill within the domain is shown in Figure 7, following Stangroom (2004) the domain size is 1900m$\times$800m$\times$900m in the x, y and z directions respectively. The meshing around the hill is created using the snappyHexMesh tool that is provided with OpenFOAM.

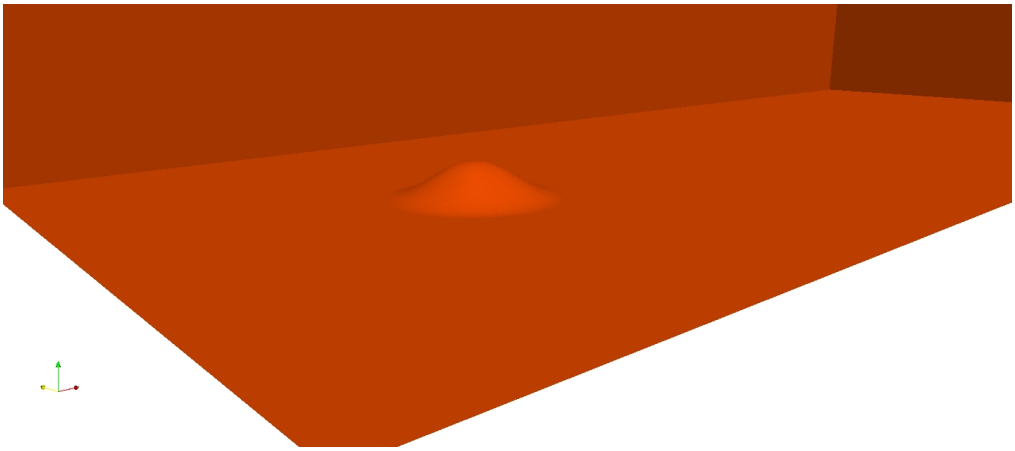

Figure 7: The cosine bump within the model domain.

The type of flow that occurs downstream of a hill like that described in (20) is well studied and so provides a good way to verify the turbulence model that is being used. A splitting of the flow in the downstream region is expected. Figure 8 shows a 2D slice in the x-z direction along the crest of the hill, the colouring in the plot denotes the x component of the wind strength. The splitting of the flow is

evident, even in this case of relatively low wind speed, there is a clear blue region in the lee of the hill with a sudden increase in wind speed at approximately the height of the hill, but decreasing further downstream of the hill. The approximate splitting appears to agree with the plots shown by Stangroom (2004).

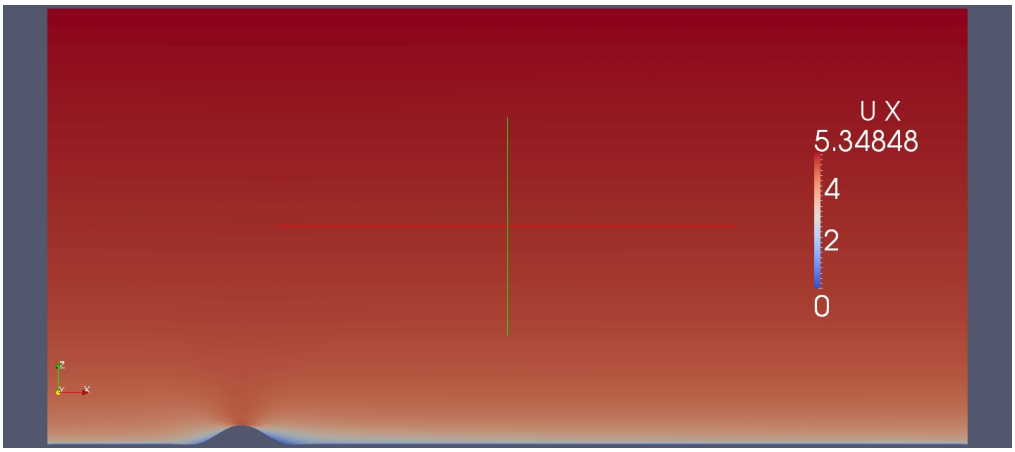

Figure 8: Two dimensional slice in the x-z direction showing the x component of the wind.

Figure 9 shows the wind speed in the vertical direction. In front of the hill there is a significant updraught and in the lee of the hill there is a significant downdraught. This effect looks as is expected and is well understood. The updraught and downdraught around a hill such as this can lead to gravity waves which can affect the flow high above the hill.

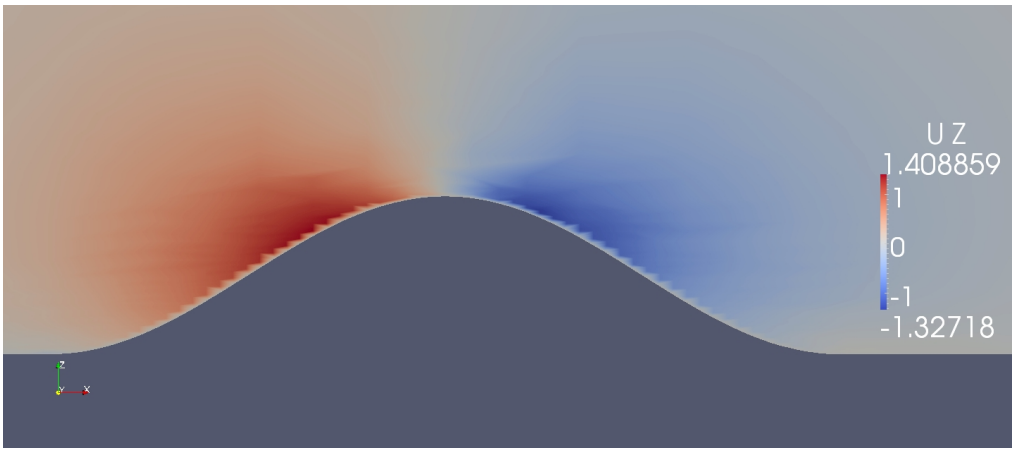

Figure 9: Two dimensional slice in the x-z direction showing the z component of the wind..

It has been beyond the scope of this project to run extensive testing of idealised test cases such as these however they would need to be completed before full confidence in a complex terrain case could be gained.

6.2 Tradewind Turbines

Once the turbulence model and the meshing has been verified by completing the downstream checks and by performing a series of idealised test cases the next step is to implement a case of complex terrain. However, as will be discussed, there will still be a number of questions that need to be considered before the model can be set up appropriately.

Tradewind Turbines is a company based in Exeter in the UK, they are a relatively new company that make vertical axis wind turbines. The turbines are designed for people and businesses that are interested in generating their own electricity on a relatively small scale. The turbine they manufacture can also be used in a portable configuration. If an accurate simulation of atmospheric wind over any given complex terrain can be generated then it would be useful for the customers of companies such as Tradewind Turbines as it would allow them to choose the most appropriate location for the turbine they have purchased. Tradewind Turbines currently have a prototype wind turbine constructed in the Devon countryside and this will be used as a test case for constructing a case of flow over a complex terrain.

6.3 Lidar Data

The initial step toward a complex terrain simulation is to generate the complex terrain itself. In the UK lidar (Light Detection And Ranging) data is available for the majority of the land area. Lidar data is available in horizontal resolutions ranging from 25cm to 2m and can be delivered in a number of formats including height levels.

The Tradewind Turbines prototype turbine is located at approximate grid reference 307000, 88000. Lidar data is available as 1km square tiles, the location of the Tradwine turbine lies close to the intersection of four tiles so all four must be obtained and later manipulated to construct a suitable domain. Unfortunately the turbine location is also located close to a region where no lidar data is available. Figure 10 shows the surrounding area for the turbine, in the figure the actual turbine location is close to the middle. Green on the figure represent where lidar data is available and blue where it is not. The red area is the area that is chosen for the terrain in the model.

As the turbine is located close to the region where no lidar data is available a region is chosen that goes as close to the region where no data is available whilst also maximising the distance between the turbine and the location where the inlet boundary condition will need to be implemented. The horizontal resolution in the lidar data is 1m.

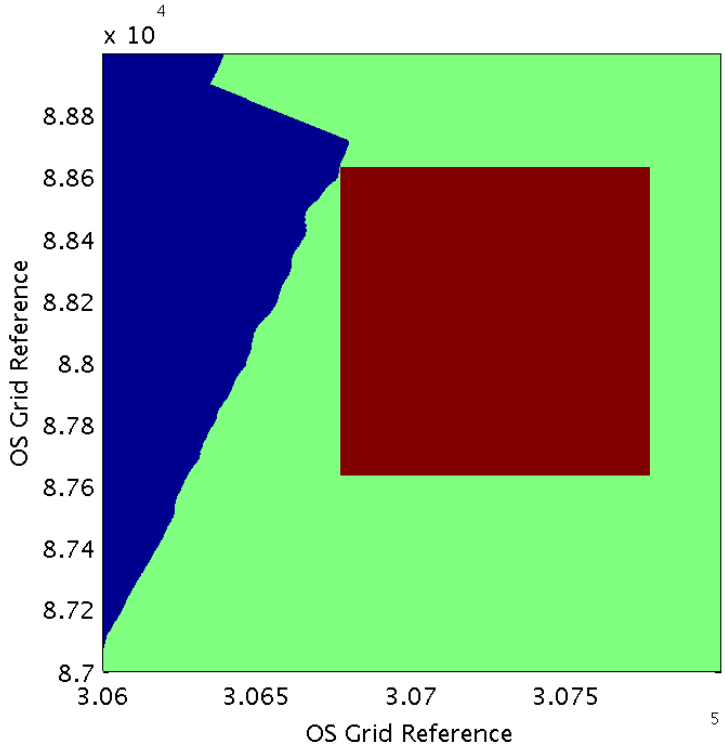

Figure 10: The surrounding area of the Tradewind Turbines prototype turbine. The different colours indicate the availability of Lidar data. Green represents the region where lidar data is available, blue represents the region where lidar is unavailable. The red area is the region that is chosen for the terrain.

6.4 STL Files

Lidar data comes as height above sea level values, if data is chosen at 1m horizontal intervals then the data can be thought of as matrix 1000×1000 in size with values as the height levels. CFD applications such as Fluent and OpenFOAM require STL (stereolithography) files, these describe a raw unstructured triangulated surface. The CFD software takes the STL file and creates a mesh around it. In order to convert from lidar to STL some coding is required. Fortunately a number of pieces of commercial and free to use software exist for conversion from lidar to STL.

Using surf2stl in Matlab and snappyHexMesh in OpenFOAM the terrain is imported and meshed. The red square that is shown in Figure 10 is now shown in its STL format in Figure 11. A close up of the turbine location is shown in Figure 12; an image of the turbine itself has been added to give an idea of scale, although the flow will not be modelled around the terrain and turbine simultaneously.

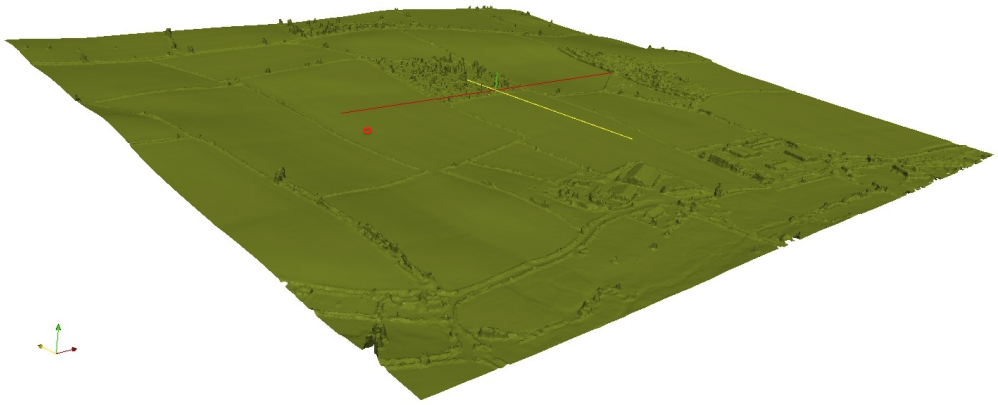

Figure 11: The terrain that will be used for the modelling. The approximate location of the turbine is shown by the small red circle. The terrain is viewed from the south west.

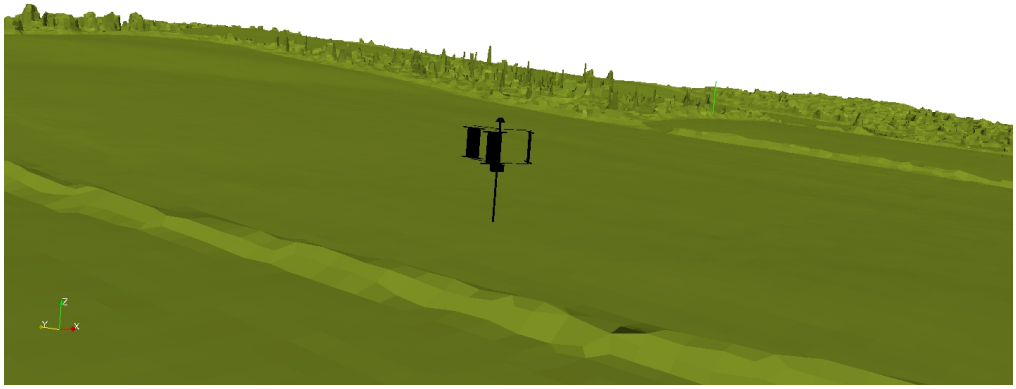

Figure 12: Close up of the turbine location within the terrain.

7 Running a Complex Terrain Case

For the terrain that will be implemented an immediate question arises; how should the inlet boundary condition be implemented? So far the inlet boundary condition that has been used is based on the logarithmic profile, the profile is based on a given friction velocity and aerodynamics roughness length. Ultimately it would be useful to construct many simulations that have the wind approaching from a multitude of directions; only then could a thorough investigation of optimal location be presented. For now the wind is considered to come from the west, this is effectively what was done for the downstream checks, also in the UK westerly and south westerly are the prevailing wind directions. In Figure 11 it is clear that at the western edge of the terrain there is quite a large range of heights and so it may not be sensible to just implement the logarithmic profile here. Certainly the wind profile would not be well developed in terms of the turbulence model by the

time it reaches the wind turbine's location.

Instead of implementing with just the size of the terrain the model domain is extended by 2km in the westerly direction. The domain can be thought of as being three sections, each 1km in length and width. In the first, most westerly, 1km by 1km the height goes from 0m everywhere along the western edge to the height of the terrain, i.e. the western edge of Figure 11. During the middle 1km by 1km the height remains constant in the east-west direction, at the height of the terrain's western edge. The third, most easterly 1km by 1km is the terrain itself. So from the most westerly edge the height increases from 0m to the height of the actual terrain at the western edge, then remains constant for 1km before coming into contact with the actual terrain. In doing this it allows the model to obtain a well developed profile before coming into contact with the terrain. Figure 13 shows the fully constructed terrain with all three segments.

Figure 13: The full model terrain with added westward slope to help produce a fully developed profile in the approach to the turbine location.

Eventually it could prove useful to allow for height variation in the inlet profile which would eliminate the need for such large domain size. It may also prove useful to examine profiles from realistic data to see what kind of inlet profile is appropriate.

Now that the domain is ready the flow simulation can be performed. The boundary conditions are largely the same as those described in the section on downstream checks, the only exception is that no-slip boundary conditions are applied at the sides of the domain since this is a full 3D simulation as opposed to the 2D simulation that was considered there. The wall functions are those described by Richards and Hoxey (1993) and the top boundary conditions are as given by O'Sullivan et al. (2011). The domain is 3000m$\times$1000m$\times$500m in the x, y and z directions respectively. The number of grid points is 120$\times$40$\times$20. The simulation is performed using simpleFOAM.

Figure 14 shows a slice in the east-west direction and along the location of the prototype turbine. Clearly the flow profile looks sensible, there is an increase with height and the values of the downstream component of the flow are within the expected range. However it is of little use to assume that the structure of the flow provides accurate insight into the flow over this terrain without the necessary study of the idealised test cases that have not been extensively examined here.

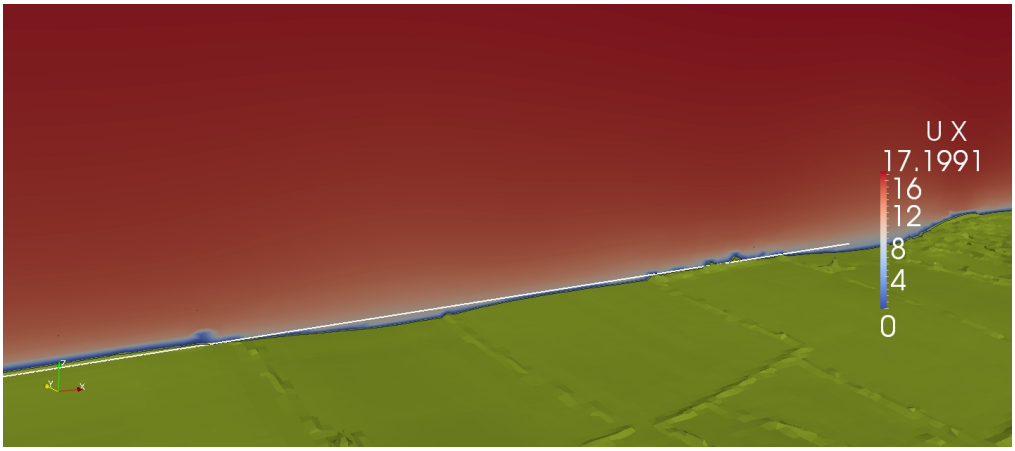

Figure 14: 2D slice along the plane at which the turbine is located showing the wind speed in the east-west direction.

OpenFOAM and the visualisation suite Paraview, that works in sync with OpenFOAM, have a number of powerful tools for examining the flow. A further useful way to visualise the flow is through the use of streamlines, an example of which is shown in Figure 15. A streamline plot helps to understand how the air will behave as it passes over hedges, trees and buildings and also helps the user to visualise where the flow may become turbulent.

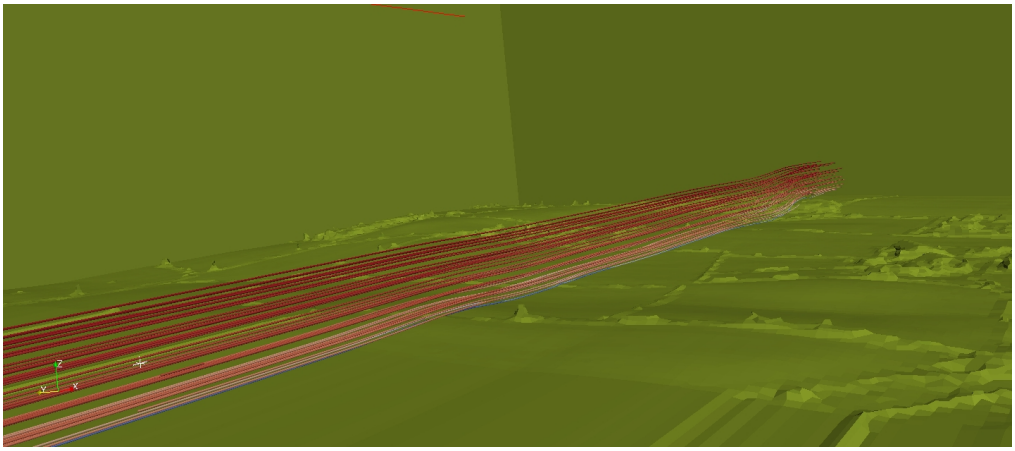

Figure 15: Streamlines of the flow across the location of the wind turbine.

8 Conclusions

The aim of this work has been to demonstrate that simulations of flow over complex terrain can be performed using OpenFOAM. The above shows that all the key steps to the implementation are possible. These can be summarised as,

- Verify that a horizontally homogeneous solution is obtained in the absence of complex terrain, and in doing so determine the most suitable way to construct the turbulence model.
- Verify the turbulence model against idealised complex terrain cases and against field experiments.
- Obtain complex terrain data from lidar data and convert to CFD friendly format such as STL.
- Create a suitable mesh for the given terrrain.
- Ensure a suitably well developed wind profile is used in the simulation.
- Perform the simulation using appropriate OpenFOAM solver.

A number of approaches for obtaining a horizontally homogeneous solution were compared and it was shown that those which used the O'Sullivan et al. (2011) consistent top boundary conditions were most successful. It was also shown that for the standard Richards and Hoxey (1993) inlet profiles the Richards and Hoxey (1993) wall functions should also be applied. The combination of the Yang et al. (2009) and O'Sullivan et al. (2011) approaches gave the most promising results but the Yang et al. (2009) approach has a general disadvantage in that the two constants need to be computed by fitting profiles to realistic data or idealised results.

A further aim of this study was to identify areas where the understanding of the various steps may be improved to gain better scientific insight from the results of the complete simulation. It has been identified that the simulation is indeed possible, however some of the steps could not been examined in detail. Before a through examination of the turbine complex terrain case is performed an extensive study of idealised complex terrain cases should be performed. The turbulence model needs to be verified for a series of ridge and valley test cases as well as for a realistic case, such as the Askervein Hill case, where actual data is available.

In addition to the need for further investigation of the flow over simplified complex terrain a number of questions have also been identified that could not be addressed within the scope of this project. These are,

- Can the turbulence model be used successfully in conjunction with a realistic inlet profile?

- Can and should the model be adapted to take stratification into account.
- Can and should the model be made to take wind turning into account?
- What kind of inlet profile should be used for the complex terrain case?

It is clear that work is still required before high levels of confidence are obtained in the full simulation. However, given how useful the full simulation would be, addressing these questions should prove very interesting.

A Flow Around a Turbine

The work in this study was performed in conjunction with Tradewind Turbines Ltd. Tradewind employ a team of CAD engineers who work on the development of the turbine. Due to the close ties with these staff it was possible to obtain STL files for the Turbine that is being built. OpenFOAM is very well suited to modelling the flow around static objects such as planes, cars, trains or motorbikes. Indeed there is a tutorial provided with OpenFOAM which models the flow around and motorbike and it's rider. This tutorial can be easily adapted to model the flow around the Tradewind Turbines turbine. Since the turbine is static it is a simplified model, the turbine will of course rotate in the wind. However it could still be a useful simulation, for example providing engineers with information about the kinds of pressures experienced by the turbine when it is switched off or when it has to be suddenly switched off in the event of a problem.

The turbine is a vertical axis turbine that has sails rather than rotor blades. These sails are electronically furled and unfurled to accommodate the strength of the wind. Figure 16 shows a simulation of the flow around the turbine when the sails are furled. The plot shows streamlines of the air flow around the turbine and the pressure for that wind speed felt on the turbine structure. Clearly with the sails furled there is little interaction between the wind and the turbine. For wind speeds of around 20ms^{-1} the turbine structure feels a pressure increase of around 200pa.

Figure 16 shows the ariflow around the turbine when the sails are completely unfurled. Normally the turbine would be turning in this situation, in this simplified case the turbine is static, however provides information for what would happen if the turbine was suddenly shut down. Clearly the flow is considerably more turbulent behind the turbine. In the streamlines the eddies downstream of the sails are evident. The pressure felt on the sails is also increased from the furled case, as would be expected.

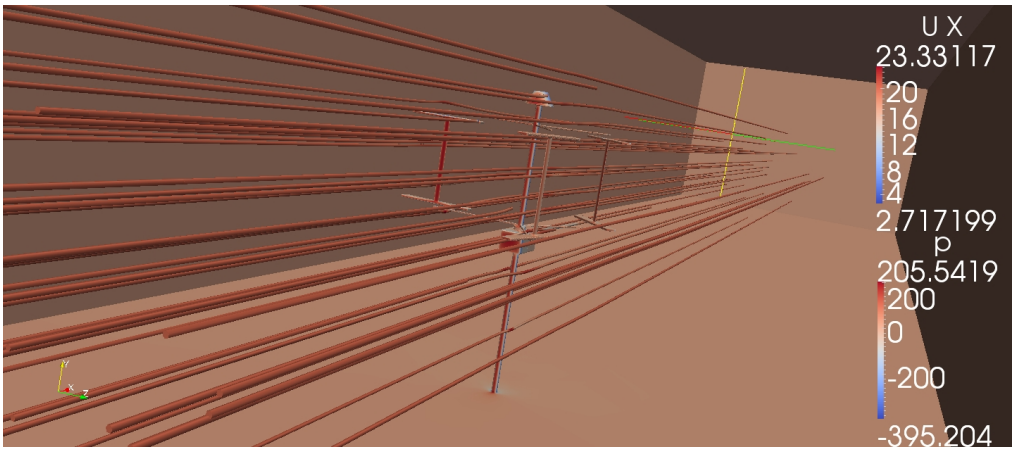

Figure 16: Airflow around the turbine when the sails are completely furled. The turbine and surface are coloured by pressure.

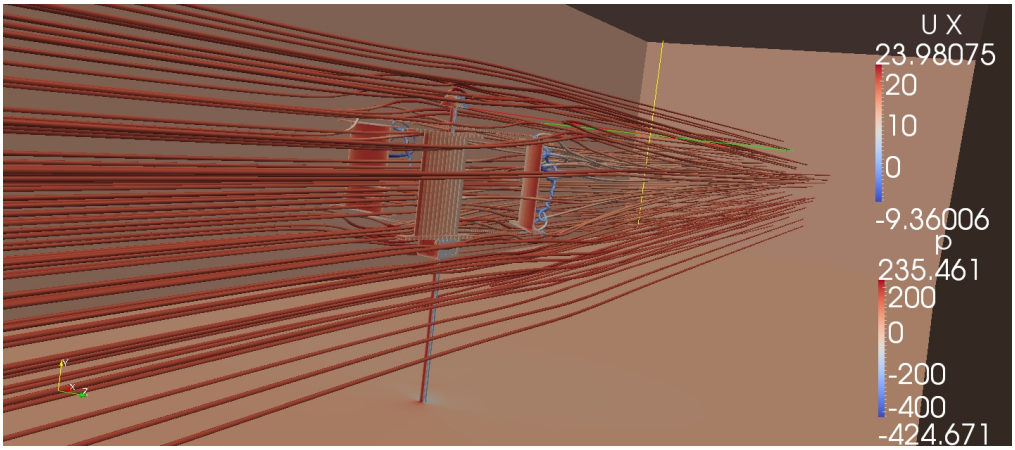

Figure 17: Airflow around the turbine when the sails are completely unfurled.

The CAD engineers can use the data from experiments such as these to perform stress tests on the turbine structure and ensure that the way it has been built will withstand the forces induced by the wind.

References

Beare, R. J. (2008). The role of shear in the morning transition boundary layer. *Boundary-Layer Meteorol.*, 129:395–410.

Beare, R. J., Edwards, J. M., and Lapworth, A. J. (2006). Simulation of the observed evening transition and nocturnal boundary layers: Large eddy simulation. *Quart. J. Roy. Meteorol. Soc.*, 132:81–99.

Bechmann, A., Berg, J., Courtney, M., Jørgensen, H., Mann, J., and Sørensen, N.

(2009). The Bolund experiment: Overview and background. Technical Report Technical Report R-1658, Risø DTU.

Beljaars, A. (1992). The parametization of the planetary boundary layer. ECMWF Course Notes.

Blocken, B., Stathopoulosb, T., and Carmeliet, J. (2007). CFD simulation of the atmospheric boundary layer: wall function problems. *Atmos. Environ.*, 41:238–252.

Franke, J., Hellsten, A., and Carissimo, B. E. (2007). Best practice guideline for the CFD simulation of flows in the urban environment. Technical report, Cost Action 732: Quatlity Assurance and Improvement of Microscale Meteorological Models.

Hargreaves, D. M. and Wright, N. G. (2007). On the use of the $k - \epsilon$ model in commercial CFD software to model the neutral atmospheric boundary layer. *J. Wind Eng. Ind. Aerod.*, 95:355–369.

Ishihara, T. and Hibi, K. (2002). Numerical study of turbulent wake flow behind a three-dimensional steep hill. *Wind Struct. Int. J.*, 5(2-4):317–328.

Ishihara, T., Hibi, K., and Oikawa, S. (1999). A wind tunnel study of turbulent flow over a three-dimensional steep hill. *J. Wind Eng. Ind. Aerod.*, 83:95–107.

Johnson, C. (2008). Summary of actual vs. predicted wind farm performance – recap of WINDPOWER 2008. 2008 AWEA Wind Resource Assessment Workshop Portland, OR.

Lock, A. P., Brown, A. R., Bush, M. R., Martin, G. M., and Smith, R. N. B. (2000). A new boundary layer mixing scheme. part i: Scheme description and single-column model tests. *Mon. Wea. Rev.*, 128(9):3187–3199.

O'Sullivan, J. P., Archer, R. A., and Flay, R. G. J. (2011). Consistent boundary conditions for flows within the atmospheric boundary layer. *J. Wind Eng. Ind. Aerod.*, 99:65–77.

Richards, P. J. and Hoxey, R. P. (1993). Appropriate boundary conditions for computational wind engineering models using the $k - \epsilon$ turbulence model. *J. Wind Eng. Ind. Aerod.*, 46:145–153.

Stangroom, P. (2004). *CFD Modelling of Wind Flow Over Terrain.* PhD thesis, The University of Nottingham.

Sumner, J. and Masson, C. (2009). Improving the $k - \epsilon$ turbulence model for simulation of atmospheric boundary layer flow.

Taylor, P. A. and Teunissen, H. (1983). ASKERVEIN '82: Report on the September/October 1982 experiment to study boundary-layer flow over Askervein, South Uist. Technical report, Meteorological Services Research Branch, Ontario, Canada.

Taylor, P. A. and Teunissen, H. (1985). The Askervein hill project: Report on the Sept./Oct. 1983, main field experiment. Technical report, Meteorological Services Research Branch, Ontario, Canada.

Vermeer, L. J., Sørensen, N., and Crespo, A. (2003). Wind turbine wake aerodynamics. *Progress in Aerospace Sciences*, 39(6-7):467–510.

Yang, Y., Gu, M., Chen, S., and Jin, X. (2009). New inflow boundary conditions for modelling the neutral equilibrium atmospheric boundary layer in computational wind engineering. *J. Wind Eng. Ind. Aerod.*, 97:88–95.